QCD minijet cross sections

Ina Sarcevic
*Theoretical Division, T-8, Los Alamos National Laboratory, Los Alamos, New Mexico 87545 and University of Arizona, Physics Department, Tucson, Arizona 85721**

Stephen D. Ellis
University of Washington, Physics Department, Seattle, Washington 98195

Peter Carruthers
University of Arizona, Physics Department, Tucson, Arizona 85721

(Received 31 October 1988)

We calculate the lowest-order QCD jet cross section for a variety of different sets of structure functions, QCD scales, and parton minimum transverse momentum $p_T^{\min}$. We compare our theoretical results with the experimental data for the jet differential and total cross sections including the minijet regime in order to study the correlations between the various parameters. We find that for a constant K factor the choice of scale $Q^2=p_T^2$ provides the best representation of the experimental data. With a K factor of order 2, a theoretical cutoff of $p_T^{\min}\sim 3$ GeV seems to describe the observed total minijet cross section with $E_T^{\rm jet}$ ($E_T^{\rm raw}$) ≥ 5 GeV. We extrapolate our results to yield predictions for the expected minijet cross section at the Fermilab Tevatron Collider which should have some resolving power to distinguish the different sets of structure functions and choices of scale.

I. INTRODUCTION

Recent UA1 results on jet cross sections at the CERN $p\bar{p}$ Collider energies ($200\leq\sqrt{s}\leq 900$ GeV) (Ref. 1) have raised the question of the applicability of perturbative QCD to low-p_T jet physics, the so-called minijet regime. The answer to this question is not immediately obvious. Higher-order perturbative contributions might be very important in this regime. The contribution to the apparent jet energy from the uncorrelated underlying event is also likely to be especially important for such events. Still the analysis of these experimental results is of considerable interest. This importance has been recognized by many theorists and some insight has already been obtained.[2] Minijets studies should also be possible at the Fermilab Tevatron ($\sqrt{s}=1800$ GeV). The results from higher energy should provide a valuable testing ground for QCD calculation as presently conducted in the leading-logarithm approximation, as well as for detailed studies of higher-order effects. Clearly the measurement of low-p_T jets provides new information about the gluon structure of the proton. The energy and luminosity of the CERN $p\bar{p}$ Collider are such that the accessible minijet p_T range corresponds to a region where gluon jets are *expected* to dominate ($x_T\leq 0.01$). Any experimental information on comparably low-p_T physics at Tevatron Collider energies will therefore have a direct impact on our knowledge of the still elusive role of the gluon. Predictions about minijets production should also be important for the design of future large detectors.

In the analysis discussed here we attempt to broaden the study of minijets by calculating the jet cross section for a range of different QCD scales, structure functions, and values of $p_T^{\min}$. We are particularly interested in the contribution to the cross section which arises from gluons relative to the one from quarks. The fact that the contribution to the cross section and therefore to multiplicities from the quarks is decreasing with energy has been used to predict interesting behavior of the multiplicity moments and the shape of the Koba-Nielsen-Olesen (KNO) scaling function $\bar{n}P_n$ (Ref. 3). The analysis of the gluon contribution to the jet cross section for large-p_T jets ($E_T^{\rm jet}\geq 50$ GeV) shows that it is increasing from $\sim 30\%$ to $\sim 60\%$ in the Collider energy range.[4] Here we focus on low-p_T minijets ($E_T^{\rm jet}\sim$ few GeV) and we want to find the energy at which the quark contribution to this minijet cross section becomes negligible. To treat these issues we must first address the uncertainties inherent in the various possible choices of structure functions, in the correlated choices of K factor and scale Q^2 and in the choice of the value of the theoretical parameter $p_T^{\min}$. These uncertainties arise for a variety of reasons.

The fact that the structure functions defined by different authors are different is a measure of both the disagreements and the gaps within the available pool of (largely deep-inelastic) data on which the detailed structure function fits are based. For the present we must simply accept and include this uncertainty in our analysis.

The assumed freedom to choose both the scale Q^2, which is used to define $\alpha_s(Q^2)$ and the structure functions, and the value of the overall multiplicative K factor is intended to represent the theoretical uncertainty due to the incompleteness of the lowest-order perturbative analysis. Since higher-order perturbative contributions can change both the normalization and the shape of the jet differential cross section, we include both an adjustable factor K and a kinematics dependent variation in the scale Q^2. Different choices for Q^2 [for example, $Q^2=(E_T^{\rm jet})^2$ versus $Q^2=\hat{s}$, the parton c.m. total energy] will change *both* the magnitude and the shape of the differential jet cross section. It should be noted, however, that the use of these parameters is only an approximation

to the uncertainty due to the missing higher-order contributions. Actually the required matrix elements are known[5] and the next-order contributions to the jet cross section will soon be understood,[6] eliminating at least a fraction of the uncertainty. Still, for the present phenomenological analysis, in the absence of more complete knowledge of the higher-order contributions, we will include both parameters. The information obtained from the analysis concerning the values of K and Q preferred by the data yields useful input to the question of the importance of the higher-order corrections at Collider energies.[7]

The qualitative relationship between the theoretical parameter $p_T^{\min}$ ($p_T^{\text{parton}} \geq p_T^{\min}$) and experimental value for $E_T^{\text{jet,min}}$ (or $E_T^{\text{raw,min}}$), which define the theoretical and experimental total minijet cross sections, respectively, can be understood by considering the definition of the standard UA1 jet-finding algorithm. This algorithm depends on two parameters: (1) an initiator threshold of 1.5 GeV and (2) distance in the pseudorapidity-azimuth plane measured relative to the initiator cell $\Delta R = \sqrt{\Delta\eta^2+\Delta\phi^2}$. The jet algorithm associates cells inside the cone $\Delta R \leq 1$ with the initiator and the total jet transverse energy becomes $E_T^{\text{jet}} = \sum E_T^{\text{cells}}$ (over cells within the cone). Such a definition clearly allows the inclusion in the E_T^{jet} of contributions arising both from a "true" parton hard-scattering process (followed by fragmentation) and from the underlying soft (and presumably uncorrelated) interactions of the "spectator" partons. Recall that in their minimum-basis event sample UA1 (Ref. 1) observes approximately $1.5/\pi$ GeV per unit area in the pseudorapidity-azimuth plane. Thus, in the absence of any correlations, a jet defined by a cone of area $\pi(\Delta R)^2 = \pi$ will receive a contribution to E_T^{jet} of order 1.5 GeV from the underlying event. There will also be sizable event-to-event fluctuations enhanced by trigger bias effects. Therefore we can expect that the theoretical value for $p_T^{\min}$ should be lower by 1–2 GeV than the experimental value for E_T^{jet}. Note also that, since the energy per unit area in the pseudorapidity-azimuth plane in minimum-bias events is observed to increase slowly with the total energy, the corresponding contribution to E_T^{jet} from (uncorrelated) soft physics should also increase with $\sqrt{s}$. For the sake of simplicity we will treat $p_T^{\min}$ as an energy-independent parameter. However, it is reasonable to expect that, for a fixed experimental E_T^{jet} threshold, $p_T^{\min}$ should actually decrease slowly as $\sqrt{s}$ increases.

Our calculations are based on the lowest-order perturbative QCD expressions for the differential and total jet cross sections:[7]

$$\frac{d\sigma_{\text{jet}}}{dy_1 dp_T} = \frac{2\pi p_T}{s} \times \int dy_2 \sum_{i,j}^{\text{partons}} [G_i(x_a,Q^2)G_j(x_b,Q^2)\hat{\sigma}_{ij}(\hat{s},\hat{t},\hat{u})] \tag{1a}$$

and

$$\sigma_{\text{minijet}}(p_T^{\text{jet}} > p_T^{\min}) = \tfrac{1}{2}\int dx_a dx_b d\cos\hat{\theta} \times \sum_{i,j}^{\text{partons}} [G_i(x_a,Q^2)G_j(x_b,Q^2)\hat{\sigma}_{ij}(\hat{s},\hat{t},\hat{u})] . \tag{1b}$$

Here y_1 and y_2 refer to the rapidities of the scattered partons and the symbols with carets refer to the parton-parton c.m. system. The summation is over all flavors i and j and the factor $\frac{1}{2}$ in front of the integral in Eq. (1b) is due to the fact that there are assumed to be 2 jets in the final state (in general this factor should account for the actual average multiplicity of jets per event). The relations between the variables $\hat{t}$, $\hat{u}$, $\hat{s}$, p_T, y_1, y_2, and $\cos\hat{\theta}$, x_a, x_b are given by

$$\hat{s} = x_a x_b s = 4p_T^2 \cosh^2\left[\frac{y_1-y_2}{2}\right], \quad \cos\hat{\theta} = \left[1-\frac{4p_T^2}{\hat{s}}\right]^{1/2} = \tanh\left[\frac{y_1-y_2}{2}\right],$$
$$x_b^a = \left[\frac{\hat{s}}{s}e^{\pm(y_1+y_2)}\right]^{1/2}, \quad \hat{t} = -\frac{\hat{s}}{2}(1-\cos\hat{\theta}), \quad \hat{u} = -\frac{\hat{s}}{2}(1+\cos\hat{\theta}) . \tag{2}$$

For the total cross section the range for $\cos\hat{\theta}$ is between $-\sqrt{1-4(p_T^{\min})^2/\hat{s}}$ and $+\sqrt{1-4(p_T^{\min})^2/\hat{s}}$ for a given $\hat{s}$ (i.e., given x_a and x_b). In Eq. (1) the $G(x,Q^2)$'s are parton distribution functions and the $\hat{\sigma}_{ij}$ are parton cross sections. In particular the required $\hat{\sigma}_{ij}$ are given by

$$\hat{\sigma}(q_iq_j' \to q_iq_j') = \frac{4\alpha_s^2}{9\hat{s}}\left[\frac{\hat{s}^2+\hat{u}^2}{\hat{t}^2}\right], \quad \hat{\sigma}(q_i\bar{q}_i \to q_j\bar{q}_j) = \frac{4\alpha_s^2}{9\hat{s}}\left[\frac{\hat{s}^2+\hat{u}^2}{\hat{s}^2}\right],$$
$$\hat{\sigma}(q_iq_i \to q_iq_i) = \frac{4\alpha_s^2}{9\hat{s}}\left[\frac{\hat{s}^2+\hat{u}^2}{\hat{t}^2}+\frac{\hat{s}^2+\hat{t}^2}{\hat{u}^2}-\frac{2\hat{s}^2}{3\hat{t}\hat{u}}\right], \quad \hat{\sigma}(q_i\bar{q}_i \to q_i\bar{q}_i) = \frac{4\alpha_s^2}{9\hat{s}}\left[\frac{\hat{s}^2+\hat{u}^2}{\hat{t}^2}+\frac{\hat{t}^2+\hat{u}^2}{\hat{s}^2}-\frac{2\hat{u}^2}{3\hat{s}\hat{t}}\right],$$
$$\hat{\sigma}(q_i\bar{q}_i \to gg) = \frac{8\alpha_s^2}{3\hat{s}}(\hat{t}^2+\hat{u}^2)\left[\frac{4}{9\hat{t}\hat{u}}-\frac{1}{\hat{s}^2}\right], \quad \hat{\sigma}(gg \to q_i\bar{q}_i) = \frac{3\alpha_s^2}{8\hat{s}}(\hat{t}^2+\hat{u}^2)\left[\frac{4}{9\hat{t}\hat{u}}-\frac{1}{\hat{s}^2}\right],$$
$$\hat{\sigma}(gq \to gq) = \frac{\alpha_s^2}{\hat{s}}(\hat{s}^2+\hat{u}^2)\left[\frac{1}{\hat{t}^2}-\frac{4}{9\hat{s}\hat{u}}\right], \quad \hat{\sigma}(gg \to gg) = \frac{9\alpha_s^2}{2\hat{s}}\left[3-\frac{\hat{u}\hat{t}}{\hat{s}^2}-\frac{\hat{u}\hat{s}}{\hat{t}^2}-\frac{\hat{s}\hat{t}}{\hat{u}^2}\right]. \tag{3}$$

The strong coupling constant $\alpha_s(Q^2)$ is given by

$$\alpha_s(Q^2)=\frac{12\pi}{(33-2N_f)\ln(Q^2/\Lambda^2)}\ , \tag{4}$$

where N_f is the number of quark flavors, Q is the scale of the interaction, and Λ is the QCD scale parameter.

The outline of the remainder of the paper is the following. Using Eqs. (1)–(4) we calculate differential and total cross sections for jet production in the Collider energy range (200 GeV $\leq\sqrt{s}\leq$ 900 GeV) and at the Tevatron energy ($\sqrt{s}=1800$ GeV) for a variety of parameter choices. The various structure-function choices considered are introduced in Sec. II. For each of these choices a value for the corresponding K factor and scale Q is determined in Sec. II A by considering large-p_T jet data (where the perturbative analysis is presumably most reliable). In Sec. II B a value of $p_T^{\min}$ is determined for each structure-function choice by considering the minijet cross-section data (with the K and Q values of Sec. II A). In this way we attempt to systematically include the effects of the theoretical uncertainties and allow the best description of the existing data for each structure function choice. With the parameters fixed we consider the energy dependence of the minijet cross section and of the various parton subprocesses in Sec. III. Finally, in Sec. IV we summarize our results and conclusions.

II. CHOICES OF STRUCTURE FUNCTIONS, K, SCALE, AND $p_T^{\min}$

First we consider the effect of different structure functions (but the same scale, K factor, and $p_T^{\min}$). The simplest choice is the UA1 parametrization of the structure functions summed over parton type and measured in large-p_T jet events characterized by $Q^2\sim 2000$ GeV^2 and $0.1\leq x\leq 0.8$. It is given by[8]

$$F(x)=G_g(x)+\tfrac{4}{9}[G_q(x)+G_{\bar{q}}(x)]$$

$$=\frac{6.2}{x}e^{-9.5x}\ . \tag{5}$$

However, the cross section calculated using this structure function with scale $Q^2=x_1x_2s$ for α_s but with *no* evolution of the structure function and with $p_T^{\min}=3$ GeV; 4 GeV; 5 GeV is too small.[9] For $p_T^{\min}=2.3$ GeV it can describe the low-energy data 200 GeV $\leq\sqrt{s}\leq$ 400 GeV, but is simply too small for $\sqrt{s}>400$ GeV. This leads us to the conclusion that we need evolved structure functions appropriate for even very-small-x values in order to study the minijet cross section over the full range of Collider energies. Thus we consider seven different evolved structure functions.

(1) Duke and Owens set 1 (Ref. 10) with a "soft-gluon" distribution and $\Lambda=200$ MeV.

(2) Duke and Owens set 2 (Ref. 10) with a "hard-gluon" distribution and $\Lambda=400$ MeV.

(3) Eichten-Hinchliffe-Lane-Quigg (EHLQ) set 1 (Ref. 11) with $\Lambda=200$ MeV.

(4) Glück, Hoffmann, and Reya[12] with $\Lambda=400$ MeV.

(5) Martin, Roberts, and Stirling set 1 (Ref. 13) with a "soft-gluon" distribution and $\Lambda=107$ MeV.

(6) Martin, Roberts, and Stirling set 2 (Ref. 13) with a "hard-gluon" distribution and $\Lambda=250$ MeV.

(7) Martin, Roberts, and Stirling set 3 (Ref. 13) with a gluon distribution which at low x behaves as $xG(x,Q_0^2)\sim 1/\sqrt{x}$ as suggested by certain theoretical considerations[14] and with $\Lambda=178$ MeV.

The Λ parameter in the structure functions is the same as in the running coupling α_s given by Eq. (4).

A. Large-p_T jets

We consider now the question of the correlation between the value of the K factor and the choice of structure function and scale Q^2. To treat this issue we compare the theoretical predictions for the inclusive jet p_T distribution, $d^2\sigma/dp_Tdy|_{y=0}$ versus p_T with the experimental data using the seven different structure functions and three choices of scale. We first focus on the high-statistics experimental data[15] for large-p_T values (where perturbation theory is presumably most reliable) at $\sqrt{s}=546$ and 630 GeV as indicated in Fig. 1. In order to simplify the plots we exhibit only the cases which exhibit the largest differences. Further we normalize all of the results to (i.e., divide all results by) the numbers obtained using structure function set 3 (Ref. 11), scale $Q^2=p_T^2$ and $K=1.5$. This choice gives an acceptable overall description of the data. We also compare our calculations to the smaller-p_T data from the ramping runs at $\sqrt{s}=200$, 500, and 900 GeV as plotted in Figs. 2, 3, and 4. The labeling scheme in these and the subsequent figures employs a two-integer label for each result. The first of the two in-

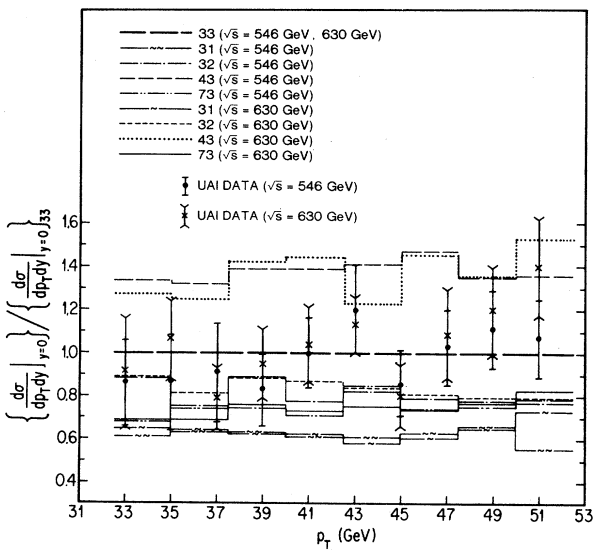

FIG. 1. Comparison between experimental data (Ref. 15) and the theoretical predictions for the p_T distribution ($d\sigma/dy\,dp_T|_{y=0}$ versus p_T) at energies $\sqrt{s}=546$ GeV and 630 GeV scaled by the 33 results with $K=1.5$. The labeling scheme is explained in the text.

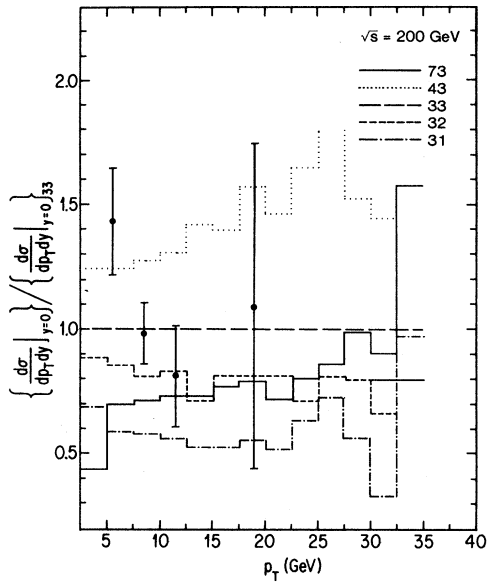

FIG. 2. Comparison between (a characteristic subset of) the experimental data (Ref. 1) and the theoretical predictions for the p_T distribution $(d\sigma/dy\,dp_T|_{y=0}$ versus $p_T)$ at energy $\sqrt{s}=200$ GeV scaled by the 33 results with $K=1.5$. The labeling scheme is explained in the text.

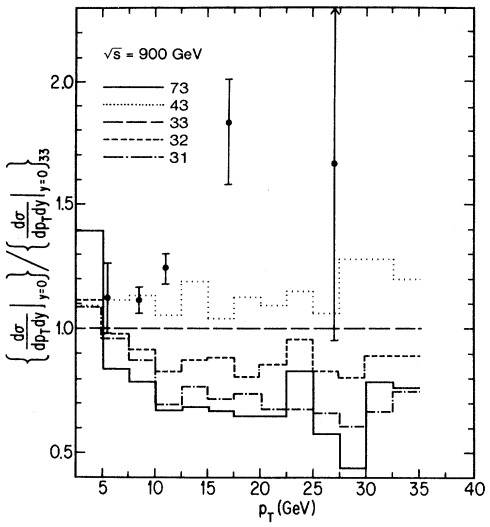

FIG. 4. Comparison between (a characteristic subset of) the experimental data (Ref. 1) and the theoretical predictions for the p_T distribution $(d\sigma/dy\,dp_T|_{y=0}$ versus $p_T)$ at energy $\sqrt{s}=900$ GeV scaled by the 33 results with $K=1.5$. The labeling scheme is explained in the text.

tegers corresponds to the number of the structure function in the list given above while the second corresponds to the choice of scale, 1 for $Q^2=\hat{s}$, 2 for $Q^2=-\hat{t}$, and 3 for $Q^2=p_T^2$. Since we have scaled all results to the 33 results (with $K=1.5$), this choice appears as the horizontal line at 1. Note that the p_T values for the data in these figures have been corrected by UA1 so that they are meant to be compared to the "true" underlying jet p_T. This correction is most reliable at the largest p_T where the theoretical predictions are likewise most reliable. The bin-to-bin fluctuations in the theoretical histograms serves to illustrate the approximately ±10% numerical uncertainty in our differential cross-section evaluation. For the present considerations this level of uncertainty is quite adequate.

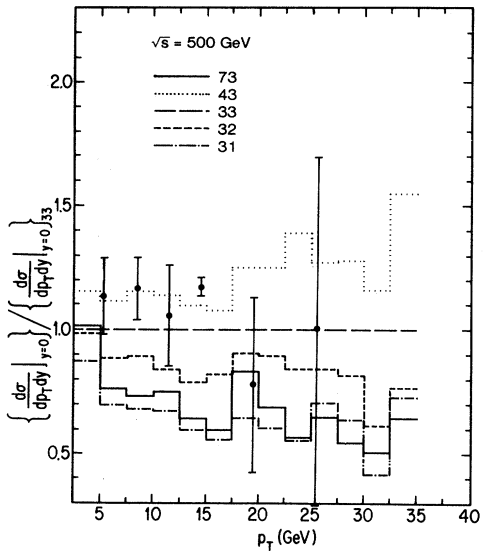

FIG. 3. Comparison between (a characteristic subset of) the experimental data (Ref. 1) and the theoretical predictions for the p_T distribution $(d\sigma/dy\,dp_T|_{y=0}$ versus $p_T)$ at energy $\sqrt{s}=500$ GeV scaled by the 33 results with $K=1.5$. The labeling scheme is explained in the text.

The K factors for the various sets of functions can be read off from Fig. 1 by determining what constant factor will bring the results for that set into agreement with set 33 and the data and then multiplying by 1.5 (the K factor for 33). From the limiting cases of 31 and 43 we see that K factor is restricted by the large-p_T data (for $\sqrt{s}=546$ GeV and 630 GeV) to be in the range from 1.1 $(=1.5\times1/1.4)$ to 2.5 $(=1.5\times1/0.6)$ with a precision for any specific choice of order 10%. We note that the large-p_T tail of the p_T distribution at $\sqrt{s}=900$ GeV is not well described by any structure function (and presumably for any choice of scale Q^2). This could be a result of experimental inconsistency since data published previously[16] do not seem to exhibit this problem. Ignoring this difficulty, it is clear that a value for K can be chosen for each of the sets of structure functions in order to yield reasonable agreement with the large-p_T data. We should note, however, that structure function set 7 with scale $Q^2=p_T^2$ does not yield a good description of the p_T distribution at low p_T at any energy. Since the contribution from the lowest bin gives the most important contribution to the integrated cross section, we can anticipate that set 7 will not yield a good description of the total minijet cross section.

By comparing the results for 31, 32, and 33 in Fig. 1 we see that the bulk of the differences at large p_T between

different choices of scale can also be absorbed into a different choice of K. From Fig. 1 we note that K factor is smaller for 33 ($K=1.5$) than for 32 ($K=1.85$) and 31 ($K=2.4$). We proceed by determining the value of K from the large-p_T data. Our choice for 33 ($K=1.5$) is in agreement with the UA1 K-factor value chosen to yield the best description of *both* minimum-bias *and* large-p_T data at $\sqrt{s}=546$ GeV and $\sqrt{s}=630$ GeV (Ref. 16).

B. Minijets

We now extend our analysis into the minijet regime as in Figs. 2, 3, and 4, and note that the *shape* in p_T of the differential cross section at small p_T is scale dependent. If we calculate the total minijet cross section of Eq. (1b) using structure function set 3 for the three choices of scale, $Q^2=\hat{s}$, $-\hat{t}$, and p_T^2 with appropriate K values (2.4, 1.85, and 1.5), we find that, in order to explain the general magnitude of this cross section we are required to make the scale-dependent choices $p_T^{\min}\sim 3.4$, 3.3, and 3.2 GeV, respectively. These values are at least qualitatively consistent with our earlier discussion of the contribution of the underlying event and with the analysis of UA1 (Ref. 1). To the extent that we can discuss minijets in this naive language, a 5-GeV minijet on average involves only a $\sim$3-GeV parton plus $\sim$2 GeV from the underlying event.

We see in Fig. 5 that this process of fixing the K value from the large-p_T data and $p_T^{\min}$ from the total minijet cross section brings the total cross section for all three scales into reasonable agreement with the data except at the lowest energy. Overall we see that the scale $Q^2=p_T^2$ seems to offer a somewhat better representation of the energy dependence of the total minijet cross section. This conclusion is in agreement with the more detailed analysis by UA1 (Ref. 17) of the angular dependence observed in large-p_T two-jet data. Data at $\sqrt{s}=1800$ GeV, where the predictions with the three different choices of scale are quite different, should serve to confirm this conclusion.

III. RESULTS

With some confidence in our chosen values of K and $p_T^{\min}$ we can now consider how the energy dependence of the total minijet cross section depends on the choice of structure function. In Fig. 6 we display the results for the seven choices of structure function, all with $Q^2=p_T^2$ and appropriate values of K and $p_T^{\min}$. As earlier we scale the data and the theoretical results by the EHLQ numbers, curve 33, which serves as our reference choice. We note that the structure functions of sets 1, 2, 3, 5, and 6 yield rather similar results (preferring only somewhat different K factors and slightly different $p_T^{\min}$). Set 2 yields a cross section which rises with energy somewhat more rapidly than 3 while set 1 rises more slowly (i.e., it falls in this scaled graph). We also note that the cross sections obtained using set 4 and set 7 exhibit the largest

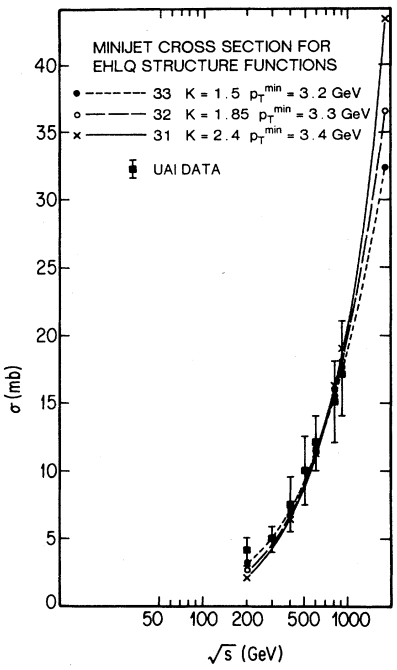

FIG. 5. Theoretical predictions for σ_{jet} obtained using EHLQ structure functions (Ref. 11) with three different scales. Set 31, $Q^2=\hat{s}$, $K=2.4$, $p_T^{\min}=3.4$ GeV (solid line); set 32 , $Q^2=-\hat{t}$, $K=1.85$, $p_T^{\min}=3.3$ GeV (long dashed line); set 33 , $Q^2=p_T^2$, $K=1.5$, $p_T^{\min}=3.2$ GeV (short dashed line). Also shown are the experimental data (Ref. 1).

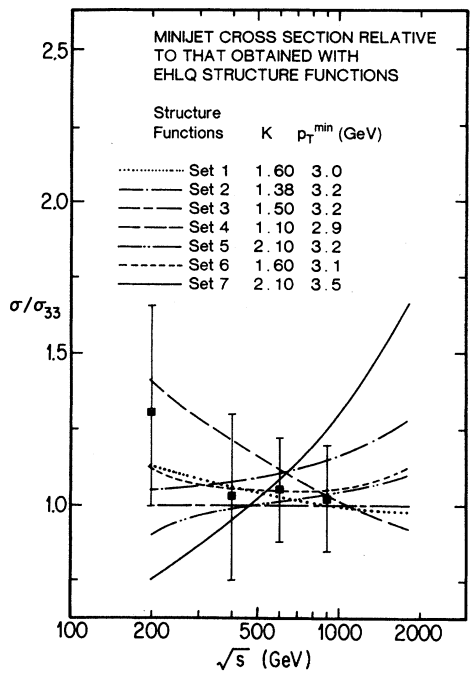

FIG. 6. Comparison between the experimental data (Ref. 1) and theoretical predictions for the minijet cross section using seven different structure functions with $Q^2=p_T^2$ and appropriate values of K and p for each set. All curves are scaled by the 33 results [EHLQ structure functions (Ref. 11), $Q^2=p_T^2$, $K=1.5$, and $p_T^{\min}=3.2$ GeV].

TABLE I. Displayed are the relative contributions from the different QCD subprocesses to the minijet cross section at energies $\sqrt{s}=200$ GeV, 500 GeV, 900 GeV, and 1800 GeV obtained with different choices of structure functions, scale, K factor, and $p_T^{\min}$. In particular, for set 31 $K=2.4$ and $p_T^{\min}=3.4$ GeV, for set 32 $K=1.85$ and $p_T^{\min}=3.3$ GeV, for set 33 $K=1.5$ and $p_T^{\min}=3.2$ GeV, for set 43 $K=1.1$ and $p_T^{\min}=2.9$ GeV and for set 73 $K=2.1$ and $p_T^{\min}=3.5$ GeV. The contributions from the subprocesses $q\bar{q}\to gg$ and $gg\to q\bar{q}$ are very small (about 0.1% and 1%–2%, respectively) and therefore these two subprocesses are not included in this table. Also shown are the UA1 (Ref. 1) minijet cross section values.

Set	qq $(q\bar{q})\to qq$ $(q\bar{q})$	$qg\to qg$	$gg\to gg$	σ_{minijet} (mb)
		$\sqrt{s}=200$ GeV ($\sigma_{\text{minijet}}^{\text{UA1}}=4\pm1$ mb)		
33	4%	35%	58%	3.01±0.01
43	7%	39%	52%	4.28±0.02
73	7%	42%	49%	2.27±0.01
		$\sqrt{s}=500$ GeV ($\sigma_{\text{minijet}}^{\text{UA1}}=10\pm2$ mb)		
33	3%	31%	64%	9.36±0.05
43	6%	37%	56%	11.02±0.07
73	5%	37%	57%	9.47±0.05
		$\sqrt{s}=900$ GeV ($\sigma_{\text{minijet}}^{\text{UA1}}=17\pm3$ mb)		
33	3%	29%	67%	17.3±0.1
43	5%	35%	58%	17.9±0.1
73	3%	34%	61%	21.7±0.1
		$\sqrt{s}=1800$ GeV		
33	2%	26%	70%	32.4±0.2
43	4%	34%	60%	29.2±0.2
73	2%	31%	64%	54.0±0.3
32	2%	27%	69%	36.7±0.2
31	2%	26%	70%	43.5±0.2

difference in energy dependence. The former increases with energy considerably more slowly than the 33 results and slightly more slowly than the data while the latter increase with energy much faster than the data. Even though set 4 can still describe the data, set 7 (with its more singular small-x behavior) is almost ruled out by the UA1 data. Experimental results at $\sqrt{s}=1800$ GeV should make this case clear. As mentioned earlier, one expects that the parameter $p_T^{\min}$ should actually be chosen to decrease slowly with increasing $\sqrt{s}$ to represent the increasing contribution to the jet from the underlying event. This will tend to magnify the differences between the various structure functions. A complete analysis of the energy dependence of the minijet cross section will require data on the energy dependence of the uncorrelated soft physics in order to accurately account for this effect.

As noted earlier, we are also interested in the question of the relative contributions of initial quarks and gluons in the minijet regime and to what extent the answer is structure-function dependent. In Table I we show that the percentage of the quark contribution relative to the gluon contribution to the cross section is decreasing with energy as expected and is negligible at the Tevatron energies for $p_T^{\min}\sim3$ GeV. This general conclusion is independent of the details of the specific structure functions used. However, if we look at the energy dependence in detail as in Fig. 7, where we plot the energy dependence of the relative contribution of $qq\to qq$, $qg\to qg$, and $gg\to gg$, we see that there are significant differences between these contributions obtained using structure function set 7 and set 4. If we wish to calculate multiplicity energy dependences in detail, this uncertainty must be kept in mind.

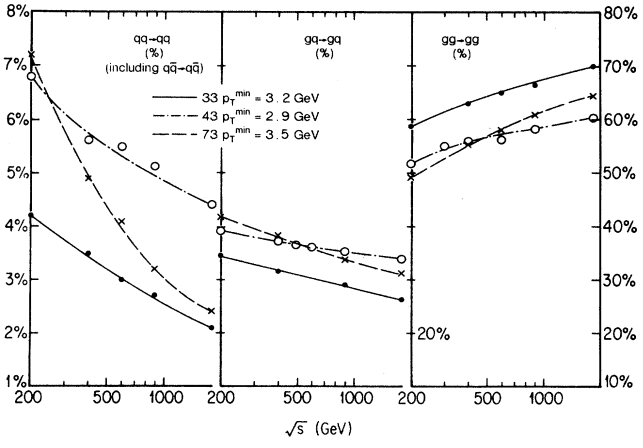

FIG. 7. Theoretical predictions for the energy dependence of the relative contribution of the following parton subprocesses: qq $(q\bar{q})\to qq$ $(q\bar{q})$, $qg\to qg$, and $gg\to gg$ obtained using structure functions given by set 3, set 4, and set 7 and appropriate values of K and $p_T^{\min}$ with $Q^2=p_T^2$.

IV. CONCLUSIONS

To summarize our analysis, we emphasize again the importance of analyzing the minijet cross section at Collider energies in the context of perturbative QCD. Such studies can provide valuable tests of the applicability of perturbative QCD to low-p_T physics. Finding the scale and the value of the K factor favored by the experimental data can also give useful input to the question of the importance of the higher-order corrections at these energies. We have indicated that to be able to describe the data we need evolved structure functions. Second, the scale $Q^2=p_T^2$ seems to be favored by the minijet data rather than the choices $Q^2=\hat{s}$ or $Q^2=-\hat{t}$. This conclusion is in agreement with previous analyses of other data. If we accept that the UA1 $E_T^{\rm jet}$ cut of 5 GeV really corresponds to a parton cut which is smaller by 1 GeV to 2 GeV (Ref. 16), then our choice of $p_T^{\rm min}\sim 3$ GeV, to explain the size of the minijet cross section, is reasonable. However, higher-order corrections are still required to explain $K>1$. On the other hand these values of K, required by the minijet data, are consistent with those obtained from consideration of the p_T distribution at large p_T. In this truly perturbative regime the data suggest that K has to be in the range $1.1\leq K\leq 2.5$ with the uncertainty correlated with differences between the various sets of structure functions. For the issue of structure-function choice, the energy dependence of the minijet cross section seems to be the important quantity. Data from the Tevatron could rule out two of the possible choices. Finally we noted that the minijet signal at the Tevatron will be dominated by initial-state gluons which could be important for multiplicity calculations. We expect that the minijet cross section at Tevatron energies should be $\sigma_{\rm minijet}=33\pm 4$ mb keeping in mind that this value is obtained by extrapolating our results from Collider energies and that the calculation does not include higher-order corrections. A better analysis of the minijet cross section will require a more precise calculation of the jet cross section and a better understanding of the relationship between the E_T measured and the theoretical cut $p_T^{\rm min}$. This would give us a better understanding of the very interesting question of the applicability of perturbative QCD to low-p_T physics.

ACKNOWLEDGMENTS

This work was supported in part by the U.S. Department of Energy, Contracts Nos. DE-AS06-88ER-40423 and DE-F602-85ER40213 and by the National Science Foundation, Contract No. PHY8217853, supplemented by funds from the National Aeronautics and Space Administration. We thank our many experimental and theoretical colleagues for useful discussions. I.S. and S.D.E. would like to acknowledge the assistance of the participants and staff at the Institute for Theoretical Physics where some of this work was performed.

---

*Permanent address.

[1]UA1 Collaboration, A. Di Ciaccio, in *Proceedings of the XVII Symposium on Multiparticle Dynamics,* Seewinkel, Austria, 1986, edited by M. Markytan, W. Majerotto, and J. MacNaughton (World Scientific, Singapore, 1986), p. 679; UA1 Collaboration, C. Albajar *et al.,* Nucl. Phys. **B309**, 405 (1988).

[2]A. H. Mueller, in *Proceedings of the Oregon Meeting,* Annual Meeting of the Division of Particles and Fields of the APS, Eugene, Oregon, 1985, edited by R. C. Hwa (World Scientific, Singapore, 1986), p. 634; G. Pancheri and Y. N. Srivastava, Phys. Lett. B **182**, 199 (1986).

[3]I. Sarcevic, Phys. Rev. Lett. **59**, 403 (1987).

[4]P. Carruthers, C. C. Shih, and Minh Duong-Van, Phys. Rev. D **28**, 663 (1983).

[5]R. K. Ellis and J. Sexton, Nucl. Phys. **B296**, 445 (1986).

[6]F. Aversa, P. Chiappetta, M. Greco, and J. Ph. Guillet, Phys. Lett. B **210**, 225 (1988); S. D. Ellis, Z. Kunszt, and D. E. Soper, Phys. Rev. Lett. **62**, 726 (1989).

[7]S. D. Ellis, in *Proceedings of the Theoretical Advanced Study Institute in Elementary Particle Physics,* Santa Fe, New Mexico, 1987, edited by R. Slansky and G. West (World Scientific, Singapore, 1988), p. 274.

[8]G. Arnison *et al.,* Phys. Lett. **136B**, 294 (1984).

[9]See the second paper in Ref. 2.

[10]D. W. Duke and J. F. Owens, Phys. Rev. D **30**, 49 (1984).

[11]E. Eichten, I. Hinchliffe, K. Lane, and C. Quigg, Rev. Mod. Phys. **56**, 579 (1984).

[12]M. Glück, E. Hoffmann, and E. Reya, Z. Phys. C **13**, 119 (1982).

[13]A. D. Martin, R. G. Roberts, and W. J. Stirling, Phys. Rev. D **37**, 1161 (1988).

[14]J. C. Collins, in *Proceedings of the Workshop on Physics Simulations at High Energies,* edited by V. Barger, T. Gottschalk, and F. Halzen (World Scientific, Singapore, 1987), p. 265.

[15]G. Arnison *et al.,* Phys. Lett. B **172**, 461 (1986).

[16]UA1 Collaboration, C. Albajar, in *Proceedings of the Workshop on Physics Simulations at High Energies* (Ref. 14), p. 39.

[17]G. Arnison *et al.,* Phys. Lett. B **177**, 244 (1986).